Coexistence of different droplet generating instabilities: new breakup regimes of a liquid filament - Supplemental Information

Michael Hein[a], Jean-Baptiste Fleury[a], and Ralf Seemann[a,b]

ESI 1: Overview

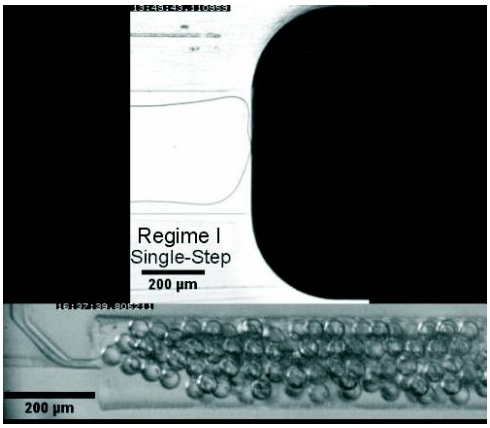

SI1: Overview of the different breakup regimes by example movies taken in the two geometries used. Top row: Geometry A ($w\backslash b$ = *30*) Bottom row: Geometry B. Movies recorded at different framerates, cf. timestamp.

ESI 2: A closer look to transitions

Regime I to II

Although only two step-instabilities were observed at a time in our experiments, it is assumed that additional step-emulsification sites can emerge on filaments with even larger aspect ratio. Using a similar device geometry with terrace aspect ratio >192 but without co-flow of continuous and dispersed phase, van Dijke et al.[1] reported droplet breakup at multiple locations evenly spaced along a filament interface with an average spacing of $\approx 25 \cdot b$. The regular distance between the breakup locations is determined by steep local pressure gradients present at the droplet breakup sites and the terrace height b, as was confirmed by CFD-simulations. The typical distance between the two droplet formation sites in our experiments is in the range of $(7\text{-}16) \cdot b$. The different spacing of droplet formation sites observed in this study presumably originates from the enhanced horizontal filament confinement with filament width always below $30 \cdot b$.

Regime II to III

Average diameters of droplets produced in regimes I to III are displayed in Fig. SI 2 to additionally support the argument of a maximum volume throughput achievable by step-instabilities causing the transition to regime III. Droplet diameters were measured directly from the recorded time series. Typically 20- 50 droplets produced by step-instabilities and 15-25 droplets produced by jet-instabilities were measured, depending on experimental conditions. The error bar denotes the standard deviation, indicating droplet polydispersity.

Within regime I and II only step-instabilities occur. Up to $Ca \approx 0.0037$, droplet diameters remain constant within experimental uncertainty, irrespective of the transition to regime II, cf. filled symbols in Fig. SI 2. At $Ca \approx 0.0037$, the droplet production frequencies of the two step-instabilities in regime II synchronize (cf. dashed line in Fig. 4 and Fig. SI 2). Simultaneously, both droplet diameters and polydispersity suddenly increase while the droplet production frequency remains about constant with increasing Ca. This sudden change of behavior indicates destabilization of the step-instabilities that reach their upper threshold of the volume throughput, which ultimately causes the transition to the next regime.
After the transition to regime III has occurred, diameters of droplets generated by step-instabilities decrease again, cf. filled diamonds in Fig. SI 2, while the maximum observed frequency of droplet production by step-instabilities remains constant, cf. Fig. 4. This indicates, that more volume over time is released by the emerging jet-instability, allowing the remaining step-instability to relax

[a] *Saarland University, Experimental Physics, Saarbrücken, Germany. Fax: +49 681 302 71700 ; Tel: +49 681 302 71777; E-mail: r.seemann@physik.uni-saarland.de*
[b] *Max Planck Institute for Dynamics and Self-Organization, Göttingen, Germany*

while operating close to its maximum frequency.
Droplets produced by jet-instabilities are significantly larger and were found to be polydisperse, as characterized in Geometry A and displayed by hollow diamonds in Fig. SI 2. This polydispersity is caused by the irregular droplet detachment due to collisions and deformations of the growing droplet by crowding in the reservoir, see also SI 1.

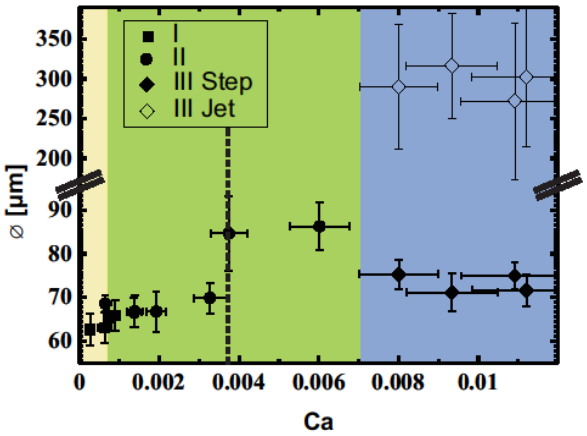

SI 2: Droplet diameter of step- and jet-instabilities. Data are mean ± SD indicating the droplet polydispersity. Data was measured at $Q_1\backslash Q_2 = 1$, i.e. for a filament width of $w_{1\infty}\backslash b = (19\pm2)$.

Regime III to IV

To further characterize the transition between regime III and IV, the growth and the retraction time of a jet with in regime III is plotted as a function of Ca_{ch} in Fig. SI 3. The retraction time represents the time of the capillarity driven retraction of the jet after droplet pinch off, whereas the growth time determines the time the jet needs to elongate before a droplet is released. The growth time is significantly reduced with increasing Ca_{ch} while the retraction time only slightly increases. Both time scales approach each other upon reaching the transition to regime IV. Presumably, the strong reduction of the growth time originates from the increased flow rate and the onset of the Rayleigh-Plateau instability. The shortening of the lifetime of jets sets an upper limit of the volume throughput a jet-instability can perform. For further increased flow rates the coexisting step-instability, which already operates at maximum frequency, switches to jetting to release more volume over time. After this transition two jet-instabilities appear on the same liquid filament and regime IV is reached.

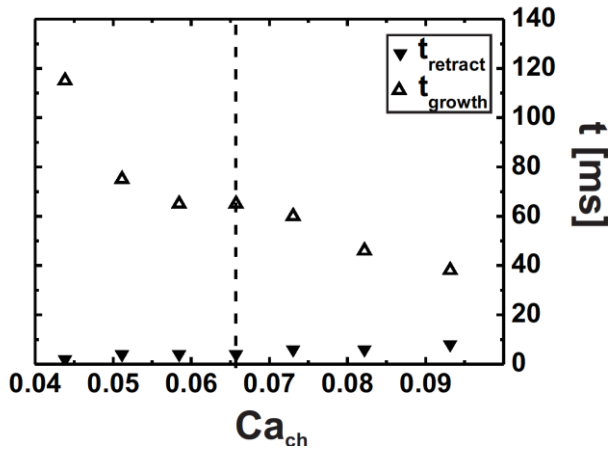

SI3: Growth and retraction times of jets in regime III as a function of Ca_{ch}. Vertical dashed line denotes $Ca_{ch} = 0.066$. Data is obtained for a fixed $Q_1\backslash Q_2 = 1.5$. Error bars are below symbol size.

ESI 3: Particle concentration

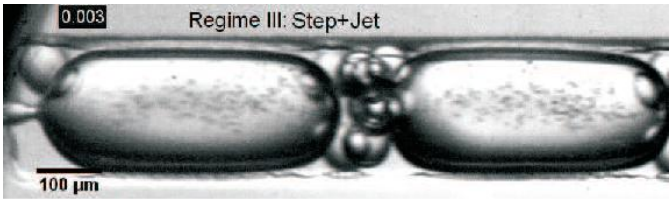

SI4: Video showing simultaneous concentration and encapsulation of PMMA particles (Ø4mm) by coexistence of step- and jet-instabilities on a single filament in Geometry B.

References

1. K. van Dijke, R. de Ruiter, K. Schroen and R. Boom, Soft Matter, **2010**, 6, 321-330.